

2005

Infrared-active phonons of perovskite $\text{HoMn}_{1-x}\text{Co}_x\text{O}_3$ ($x=0-0.8$)

F. Gao

University of Wollongong

X. L. Wang

University of Wollongong, xiaolin@uow.edu.au

M. M. Farhoudi

University of Wollongong

R. A. Lewis

University of Wollongong, roger@uow.edu.au

Publication Details

This article was originally published as: Gao, F, Wang, XL, Farhoudi, MM and Lewis, RA, Infrared-active phonons of perovskite $\text{HoMn}_{1-x}\text{Co}_x\text{O}_3$ ($x=0-0.8$), IEEE Transactions on Magnetics, October 2005, 41 (10), 2763-2765. Copyright IEEE 2005.

Infrared-Active Phonons of Perovskite HoMn_{1-x}Co_xO₃ (x = 0–0.8)

F. Gao, X. L. Wang, M. M. Farhoudi, and R. A. Lewis

Institute for Superconducting and Electronic Materials, University of Wollongong, Wollongong NSW 2522, Australia

Polycrystalline perovskites compounds HoMn_{1-x}Co_xO₃ (x = 0–0.8) have been prepared by conventional solid-state reaction. Here, we used far-infrared (FIR) spectroscopy to study infrared active phonon modes and present a comparative analysis of infrared transmission spectra of polycrystalline HoMn_{1-x}Co_xO₃ (x = 0–0.8). The data indicated that phonon modes significantly changed with increase of cobalt doping level. Four main bands were assigned as external, torsional, bending and stretching bands. The external vibration energy remain same at $\omega_1 \sim 190 \text{ cm}^{-1}$ for Co doping $x \leq 0.5$ and shift to higher energy for $x > 0.5$. Torsional and bending bands exhibit splitting. The stretching band is at 600 cm^{-1} for all samples, but the bandwidth is reduced as Co doping increased. The transmission spectrum of HoMn_{4/5}Co_{1/5}O₃ was analyzed to obtain the spectrum of optical density. The minimum number of oscillators to obtain a reliable fit is 5 by using a sum of noninteracting harmonic oscillators.

Index Terms—Far-infrared spectroscopy, perovskites, phonon modes.

I. INTRODUCTION

PEROVSKITE containing rare-earth and transitional metal cations on A and B sites (with general formula ABO₃) is a class of material which exhibits interesting and useful electronic and magnetic properties. Distortions from the ideal cubic structure can occur by concerted rotation of BO₆ octahedra, or by displacement of the A and B cations in their sites. These distortions usually result in a lowered symmetry and changed unit cell sizes. Such perovskite distortion also leads to dramatic changes in the electronic and magnetic properties. The cobaltite/manganite perovskites A(Mn_{0.5}Co_{0.5})O₃, where A is a lanthanide, exhibit ferromagnetism. The ferromagnetism arises from the superexchange interaction between Co²⁺ and Mn⁴⁺ ions mediated by oxygen [1]. The Curie temperature, T_C, is relatively high and decreases systematically with decreasing radius of the ion on the A site. The magnetic behavior of rare-earth cobaltite/manganite perovskite compounds is therefore seen to be intimately related to their structure. The magnetic behavior of A(Mn_{0.5}Co_{0.5})O₃ compounds having larger ions (La, Pr, Nd, Sm, Eu) and those having smaller ions (Gd, Tb, Dy, Y, Ho) on the A site has been investigated [2]. The spin glass magnetism resulting from the competing ferromagnetic and antiferromagnetic exchange interaction has been observed in many manganese and cobalt-based compounds [3]–[5]. One can expect a competition between ferromagnetic Co³⁺-Co⁴⁺ or Mn³⁺-Mn⁴⁺ and antiferromagnetic Co³⁺-Co⁴⁺ or Mn³⁺-Mn³⁺ (or Mn⁴⁺-Mn⁴⁺) interaction for Co and Mn based spin glass compounds. The spin glass can arise from a frustration of the competition [6]. Also, phonon modes and phonon energies in cobaltite/manganites have been determined by far-infrared spectroscopy. The phonon energies systematically shift and split, and new modes appear as the mass of the lanthanide is increased through the series A = La, Nd, Dy, Ho, Yb. This behavior of the phonon modes correlates with the magnetic properties of this series of compounds, in

particular with the appearance of metamagnetism for the compounds with smaller ions on the A site [7].

In this work, we investigated the phonon modes of HoMn_{1-x}Co_xO₃ (x = 0–0.8) perovskites by FIR spectroscopy.

II. EXPERIMENT

Perovskite polycrystalline samples HoMn_{1-x}Co_xO₃ (x = 0, (1/5), (1/3), (1/2), (2/3), (4/5)) were synthesized by the standard solid-state reaction method. Appropriate amounts of Ho₂O₃, Mn₂O₃ and CoCO₃ were mixed and sintered at 900 °C in air with intermediate grinding then pressed into a pellet. A final sintering process step was carried out at 1400 °C. The structures of HoMn_{1-x}Co_xO₃ were characterized by XRD using Philips diffractometer with CuK α radiation. The magnetic properties were investigated at temperatures between 4.2 and 300 K using a Quantum Design Physical Property Measurement System (PPMS). For infrared transmission measurement, the polycrystalline samples diluted in CsI have been finely milled and pressed into pellets. The transmission experiment was carried out using a Bomem DA3.26 rapid scan interferometer with a DTGS detector that has a range between 10 and 700 cm⁻¹. The experimental resolution and scan speed were 4 cm⁻¹ and 0.2 cm⁻¹/s, respectively. We performed measurements on the HoMn_{1-x}Co_xO₃ samples at room temperature. The intensity $I(\omega)$ is the transmitted intensity through the pellet containing the holmium manganese oxide and $I_0(\omega)$ is the transmitted intensity through a pure CsI pellet.

III. RESULTS AND DISCUSSIONS

For the samples with x = 0–0.8 doping level, X-ray diffraction show that structures are orthorhombic and HoMnO₃ is hexagonal. The lattice parameter increases as Co doping level decreases for HoMn_{1-x}Co_xO₃ (x = (1/5), (1/3), (1/2)). The ferromagnetism are gradually suppressed when doping level greater and less than x = 0.5. The details of structures and electronic and magnetic properties of HoMn_{1-x}Co_xO₃ will be discussed in [8].

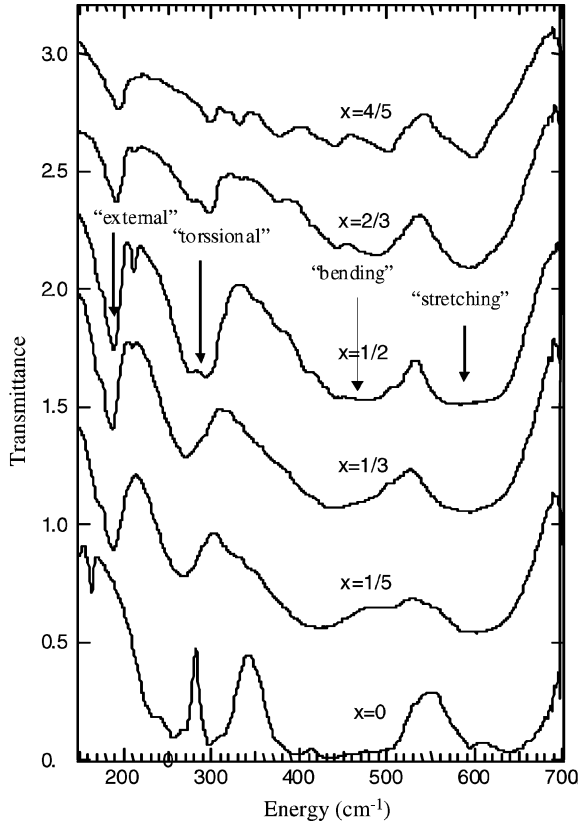


Fig. 1. FIR transmission spectra of doping-dependent for $\text{HoMn}_{1-x}\text{Co}_x\text{O}_3$ ($x = 0-0.8$) crystalline samples at room temperature.

Fig. 1 shows doping-dependent transmission spectra (ratio of $I(\omega)/I_0(\omega)$) of $\text{HoMn}_{1-x}\text{Co}_x\text{O}_3$ ($x = 0-0.8$) at room temperature in the range $150-700 \text{ cm}^{-1}$. It should be noted that we were not able to obtain the same range as the detector because CsI is opaque at lower frequencies [9]. The optical modes of the ideal cubic structure have the irreducible representation $\Gamma = 3F_{1u}$ (infrared active) + F_{2u} (infrared inactive). Thus threefold degenerate infrared active modes are expected for wave-vector $\mathbf{k} = 0$. Last [10] identifies the bands in order of increasing energy as external A-(BO_3) vibration, O-B-O bending, and B-O stretching. As the crystal symmetry is reduced, more optical modes are expected. There are 25 infrared active modes for orthorhombic (D_{2h}^{16} , Pnma) symmetry [11]. In particular, the forbidden torsional mode $F_{2u}(\text{O}_h^1)$ is now allowed and has been calculated to lie between the external and bending modes [12]. In view of the big difference noted in the transmission spectrum of HoMnO_3 which is hexagonal in Fig. 1, we will now concentrate on the spectra of $\text{HoMn}_{1-x}\text{Co}_x\text{O}_3$ ($x = 0.2-0.8$). The phonon modes of $\text{HoMn}_{0.5}\text{Co}_{0.5}\text{O}_3$ are the same as [7] observed. Consequently, the four broad bands for $\text{HoMn}_{0.5}\text{Co}_{0.5}\text{O}_3$ are assigned to: external band at $\omega_1 \sim 190 \text{ cm}^{-1}$ and weaker bands are seen to develop on either side ($\sim 160 \text{ cm}^{-1}$, $\sim 210 \text{ cm}^{-1}$); torsional band is at $\omega_2 \sim 280 \text{ cm}^{-1}$ and splits into two; bending band is located at $\omega_3 \sim 450 \text{ cm}^{-1}$ and stretching band is broadened, at $\omega_4 \sim 600 \text{ cm}^{-1}$. The behavior of the four main bands of $\text{HoMn}_{1-x}\text{Co}_x\text{O}_3$ with Co doping-dependence is as follows. The external vibration energy remains at $\omega_1 \sim 190 \text{ cm}^{-1}$ for Co doping $x \leq 0.5$ and shifts to higher energy for $x > 0.5$,

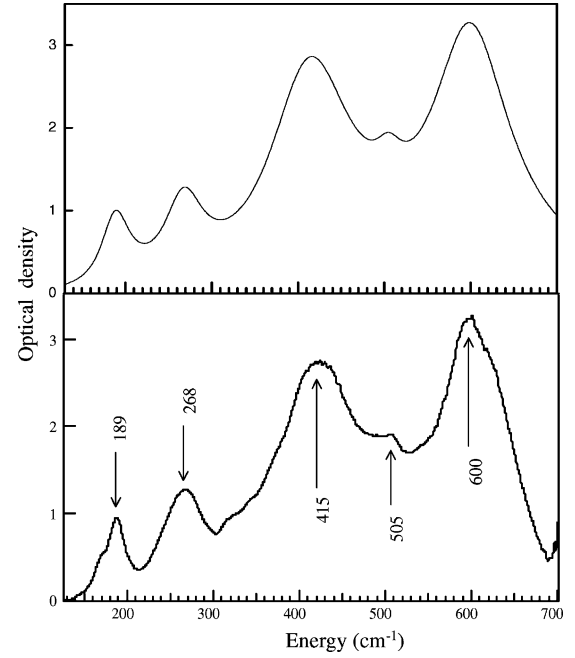


Fig. 2. Normalized optical density of polycrystalline $\text{HoMn}_{4/5}\text{Co}_{1/5}\text{O}_3$. The bottom curve is analyzed from experiment data. The top panel represents the best fit according to (1).

the weaker band $\sim 210 \text{ cm}^{-1}$ formed from $x = 1/3$ and disappeared at $x = 4/5$. The disappearance of a subsidiary band at lower energy ($\sim 160 \text{ cm}^{-1}$) accounts for the increasing energy of the main external band as Co doping increasing. The stretching band is at $\omega_4 \sim 600 \text{ cm}^{-1}$ for all samples but the band's width is reduced as Co doping increased.

The bending mode shows the most dramatic behavior. The dependence of the bending and stretching modes, related respectively to the B-O distance and the B-O-B angle, on the radius of the ion on the A site, and the effect on the infrared spectrum have been discussed by Arulraj and Rao [13] in the context of the $\text{Ln}_{1/2}\text{A}_{1/2}\text{MnO}_3$ compounds. As the radius of the ion on the A site decreases, the distance B-O increases while the angle B-O-B decreases. Increasing the B-O distance should decrease the energy of the stretching mode. Both stretching and bending modes would be sensitive to octahedral distortion and the associated lowering of symmetry arising from charge-ordering or the Jahn-Teller effect. This would result in splitting of these bands. More splitting in bending also in torsional bands are observed.

Fig. 2 shows the normalized optical density spectrum of $\text{HoMn}_{4/5}\text{Co}_{1/5}\text{O}_3$. The bottom panel depicts the measured optical density, $O_d(\omega) = \ln[I_0(\omega)/I(\omega)]$. The spectrum exhibits peaks at energies associated with the infrared active phonon modes. To extract information on phonon energies we fit the spectrum of optical density using a sum of noninteracting harmonic oscillators. It has been shown [9], [14], [15] that in the first approximation the normalized spectrum of optical density $O_d(\omega)$ is proportional to the optical conductivity $\sigma(\omega)$. By taking this into account, the equation can be written as

$$O_d(\omega) = \sum_j \frac{S_j \omega^2 \gamma_j}{(\omega_j^2 - \omega^2) + \gamma_j^2 \omega^2} \quad (1)$$

where ω_j , γ_j and S_j are frequency, width and oscillator strength of j th oscillator, respectively. The minimum number of oscilla-

TABLE I
BEST-FIT VALUES OF FREQUENCIES (ω_j), WIDTHS (γ_j), AND AMPLITUDES (S_j) EXTRACTED FROM MEASURED PHONON PEAKS (FIG. 1 BOTTOM PANEL)

ω_j	189	268	415	505	600
γ_j	40	55	118	39	100
S_j	0.34	0.52	3.1	0.15	3.2

tors to obtain a fit is 5 for $\text{HoMn}_{4/5}\text{Co}_{1/5}\text{O}_3$. In Fig. 2, the top panel is the calculation using (1) and resulting phonon frequencies are shown. In Table I, we listed the best fit-values of ω_j , γ_j , and S_j from measured phonon peaks.

IV. CONCLUSION

We have reported the infrared transmittance spectra of polycrystalline samples of $\text{HoMn}_{1-x}\text{Co}_x\text{O}_3$ ($x = 0, (1/5), (1/3), (1/2), (2/3), (4/5)$). The phonons of $\text{HoMn}_{4/5}\text{Co}_{1/5}\text{O}_3$ were measured and analyzed. It is found that the oscillator strength is predominantly carried by two modes at 415 cm^{-1} and 600 cm^{-1} . It should be pointed out that the further studies of temperature-dependent FIR spectroscopy will be performed on some of these samples.

ACKNOWLEDGMENT

This work was supported by the Australian Research Council under Discovery Grant DP0345012 (X. L. Wang).

REFERENCES

- [1] G. Blasse, *J. Phys. Chem. Solids*, vol. 26, pp. 1969–1971, 1965.
- [2] I. O. Troyanchuk, N. V. Samsonen, and E. F. Shapovalova, *Mater. Res. Bull.*, vol. 32, no. 1, pp. 67–74, 1997.
- [3] A. Sundaresan, A. Maingan, and B. Raveau, *Phys. Rev. B*, vol. 55, pp. 5596–5599, 1997.
- [4] J. Perez, J. Garcia, J. Blasco, and J. Stankiewicz, *Phys. Rev. Lett.*, vol. 80, pp. 2401–2404, 1998.
- [5] D. Groult, C. Martin, A. Maignan, D. Pelloquim, and B. Raveau, *Solid State Commun.*, vol. 105, pp. 583–588, 1998.
- [6] X. L. Wang, M. James, J. Horvat, F. Gao, A. H. Li, H. K. Liu, and S. X. Dou, *J. Magn. Magn. Mater.*, vol. 246, pp. 86–92, 2002.
- [7] F. Gao, R. A. Lewis, X. L. Wang, and S. X. Dou, *J. Solid State Chem.*, vol. 160, pp. 350–352, 2001.
- [8] X. L. Wang and M. Farhoudi, in preparation.
- [9] A. Paolone, P. Giura, P. Calvani, P. Dore, S. Lupi, and P. Maselli, *Physica B*, vol. 244, pp. 33–40, 1998.
- [10] T. Last, *Phys. Rev.*, vol. 105, pp. 1740–1750, 1957.
- [11] Q. Williams, P. R. Jeanloz, and P. McMillan, *J. Geophys. Res.*, vol. 27, pp. 8116–8128, 1987.
- [12] I. Nakagawa, A. Tsuchida, and T. Shimanouchi, *J. Chem. Phys.*, vol. 47, pp. 982–989, 1967.
- [13] A. Arulraj and C. N. R. Rao, *J. Solid State Chem.*, vol. 145, pp. 557–563, 1999.
- [14] P. Calvani *et al.*, *Phys. Rev. Lett.*, vol. 81, pp. 4504–4507, 1998.
- [15] I. Fedorov, J. Lorenzana, P. Dore, G. De Marzi, p. Maselli, and P. Calvani, *Phys. Rev. B*, vol. 60, pp. 11 875–11 878, 1999.

Manuscript received February 7, 2005.